Compliant manipulator design method (COMAD) for the type synthesis of all serial and parallel multi-DoF compliant mechanisms, with example of a Schönflies motion generator

Huisjes, A. E.; van der Wijk, V.

DOI
10.1016/j.mechmachtheory.2023.105342

Publication date
2023

Document Version
Final published version

Published in
Mechanism and Machine Theory

Mechanism and Machine Theory 186 (2023) 105342

Contents lists available at ScienceDirect

Mechanism and Machine Theory

journal homepage: www.elsevier.com/locate/mechmt

Research paper

Compliant manipulator design method (COMAD) for the type synthesis of all serial and parallel multi-DoF compliant mechanisms, with example of a Schönflies motion generator

A.E. Huisjes *, V. van der Wijk

Precision and Microsystems Engineering Department, Delft University of Technology, 2628CD, Delft, The Netherlands

ARTICLE INFO

Keywords:
Synthesis method
Parallel compliant mechanisms
Multi-DoF flexure systems
Spatial motion

ABSTRACT

This article presents the compliant manipulator design method (COMAD) for the synthesis of serial and parallel multi-DoF compliant mechanisms. Currently, the freedom and constraint topology (FACT)-method results in flexure systems being a serial kinematic solution for multi-DoF motions. In the COMAD method parallel solutions are included too through 3 steps: (1) obtaining the serial and parallel kinematic solutions for an intended set of end-effector DoFs with the *type synthesis of legs-method*; (2) transforming each legtype into a flexure leg by using the *FACT* method; (3) combining legs in parallel to obtain complete compliant mechanism designs. It was applied for a compliant Schönflies motion generator – having three translations and one rotation – resulting in 5 different 4-DoF flexure legs. 4 designs were new compared to the result obtained using the FACT method. Then, a set of legs was combined in parallel resulting in a compliant Schönflies mechanism, which was manufactured. Its mobility was experimentally evaluated by modal analysis. The intended motions separately became visible during its first four eigenmodes. They are the mechanism's DoFs as their stiffness is relatively low.

1. Introduction

Compliant mechanisms are advantageous as compared to rigid body mechanisms because they exhibit excellent repeatable motion, and have a lower part count, mass, and costs since their motion rely on the elastic deformation of their slender segments instead of a relative motion between two bodies of a rigid joint [1–4]. Moreover, compliant mechanisms require no lubrication, an important requirement for the ultra-clean environments of the precision mechatronics or food handling industries. However, because of their performance limitations, they are not widely applied yet. For instance, their range of motion (RoM) generally is limited as material stresses increase and constraint stiffnesses decrease significantly during deformation [5,6].

Compliant mechanisms are often designed with the rigid body replacement method (RBR) or the freedom and constraint topologies method (FACT) [2]. Aside, some other methods are regularly used like the constraint-based method [7], the screw-theory-based method [8,9], the constraint and position identification approach [10], and the constraint-flow-based method [11]. Those methods have been briefly elaborated and compared in [11] and together with the RBR method and FACT method they have resulted in a variety of compliant designs [2,6,12,13]. Here we will elaborate on the latter two methods.

The RBR method and the FACT method are mainly used in the conceptual phase for designing compliant mechanisms. They do not inherently consider the actuation of the mechanisms but are used as type synthesis to obtain possible non-driven mechanical

* Corresponding author.
E-mail address: a.e.huisjes@tudelft.nl (A.E. Huisjes).

https://doi.org/10.1016/j.mechmachtheory.2023.105342
Received 10 November 2022; Received in revised form 13 February 2023; Accepted 22 March 2023
Available online 10 April 2023

structures that allow for certain motions and constrain other motions between two connected rigid bodies. With the RBR method, the joints of a given rigid body mechanism are replaced individually with a representative compliant joint. The mechanical behavior then can be analyzed using a Pseudo Rigid Body Model (PRBM) [1]. Comparison, using the FACT method the end-effector motion and the complete mechanism are considered altogether. Multi-degree-of-freedom (DoF) flexure systems are synthesized by means of a complementary pair of freedom and constraint spaces [2,14,15]. Here the freedom-space determines the mechanism's internal DoFs, which is equal to the end-effector DoFs, and the constraint space determines the layout of the flexure system. The constraint space comprises a topology of parallel constraint lines with specific directions and determines how constraints could be placed between two rigid bodies for moving properly. Each constraint line represents a wire flexure and subsequently results in the possible layouts of the flexure mechanism. For the user, both methods are straightforward to apply as no prior knowledge about rigid linkage synthesis is requested as one can use existing compliant joints or use the FACT library wherein all existing freedom and constraint spaces are documented. For applications with a few DoF such as planar motion applications, positioning stages, and multi-DoF flexure joints both methods perform well [2,16,17] as their results are compact.

However, multi-DoF compliant mechanisms with spatial motion are seldom designed with these methods as it results in bulky designs. As an example, a typically desired spatial motion is the Schönflies motion whereby the end-effector possesses a combination of three translations and one rotation [18], often required in robotic manipulator applications. Utilizing the RBR method for multi-DoF spatial motion patterns result in a linkage, either serial or parallel, of rigid links and all large compliant joints which makes the design rather heavy and bulky. The solution space is limited because the kinematics of the joints are considered individually.

Using the FACT method, the obtained designs are generally more compact than for the RBR method, however, its solutions space is still limited and it results in mechanisms with multiple flexure topologies in series for most multi-DoF spatial motion patterns. Mechanisms of a single flexure topology can solely be obtained for the 26 different motion patterns that are included in the FACT library and these are mainly planar or comprise 3 rotations. For other motions, such as those with a combination of three translations, a single flexure topology is not obtained since one of the end-effector's translational DoFs is already constrained once the first wire flexure connects it to the ground [15,19]. As a consequence, they are obtained by dividing the requested end-effector DoFs into subsets, finding a complementary pair of freedom and constraint spaces for each of them, and consecutively assembling multiple flexure topologies in series by connecting them with an additional intermediate body [20]. In essence, those obtained designs are essentially a serial kinematic solution as they are an open serial chain with internal DoFs equal to the end-effector's DoFs. For them, the FACT method provides all designs. However, parallel kinematic solutions are not considered as the FACT method can only be applied to open serial kinematic chains by considering both the end-effector motion and the complete mechanism altogether. Therefore, it cannot be used that obviously for parallel mechanisms as they have a closed kinematic chain with coupling among their legs that have different kinematics than the end effector. Using the FACT method, limits to only a single kinematic solution while parallel mechanisms provide a large diversity of possible kinematic solutions, especially for spatial motion patterns [18,21].

The goal of this article is to present and show the potential of the compliant manipulator design method (COMAD); a design method for the type synthesis of serial and parallel multi-DoF compliant mechanisms considering the kinematics of the complete mechanism as a single multi-DoF flexure mechanism.

First, the theory of the COMAD method is presented in Section 2. Subsequently, in Section 3, the potential of the method is illustrated by the synthesis of all 4-DoF flexure legs for a Schönflies motion pattern and a full parallel compliant design is presented. The development of a demonstration prototype of this design is described in Section 4. In Section 5, an experiment is presented to evaluate the DoFs of the demonstrator and the results are presented in Section 6. In Section 7, the obtained flexure designs and the observed mechanical characteristics of the demonstrator are discussed and recommendations for future research are given. The conclusions are presented in Section 8.

2. The COMAD method

Fig. 1 presents a schematic overview of the process of the COMAD method which has three steps. The process starts at the top of Fig. 1 by defining the set of intended end-effector DoFs, $\mathcal{F}_e = i\boldsymbol{T} - j\boldsymbol{R}$, i.e. the required motion pattern of the compliant mechanism (or its instantaneous mobility). Here $i\boldsymbol{T}$ are the number of translational DoFs, and $j\boldsymbol{R}$ the number of rotational DoFs; where i and j are counters from 0 till 3. Then in step 1 kinematic leg solutions are obtained which in step 2 are transformed into flexure leg designs and subsequently combined to complete mechanism concept solutions in step 3. The steps will now be explained in detail.

Step 1: Kinematic leg solutions

In step 1, the kinematic solutions are obtained by using the *Type synthesis of Legs*-techniques by Kong et al. [18]. This method results for a required motion pattern in a table with all the kinematic solutions. Each kinematic solution synthesized independently and is called a leg which is an open serial mechanical linkage with rigid links and a different number of prismatic and revolute joints in a yet undetermined order. Each leg topology is noted in the documented tables by the number of prismatic and revolute joints in the linkage. Parallel kinematic solutions need to be coupled in parallel to the end-effector. In addition, geometrical conditions are given belonging to the leg types. They specify the permitted positions and orientations of the leg's joints pertaining to the end effector. In a parallel mechanism, all constraints acting on the end-effector are equal to the sum of the constraints present in the legs. So, when the legs are coupled in parallel their joints and constraints must be positioned and orientated such that they are aligned with the desired motion and constraint directions for the end-effector. Proper alignment is guaranteed when the geometrical conditions are satisfied when assembling the legs.

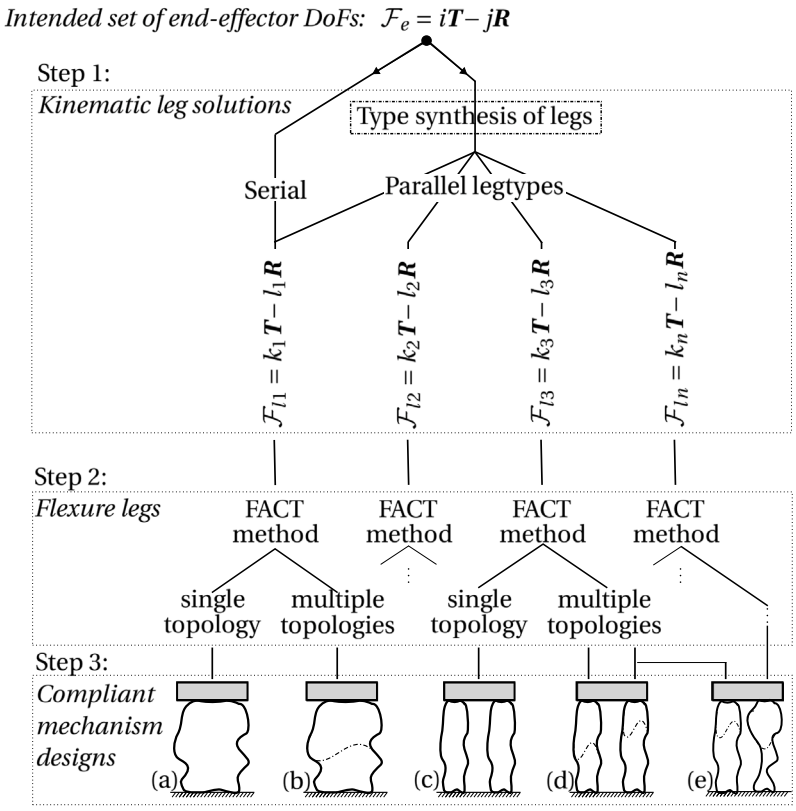

Fig. 1. Schematic overview of the COMAD method: The process starts at the top by defining the set of end-effector DoFs, $\mathcal{F}_e$. Then in step 1 the kinematic leg solutions (the serial and parallel ones) are obtained using the *Type synthesis of legs* method. In step 2 are those transformed into flexure leg designs of a single or multiple serial stacked topologies using the *FACT* method. In step 3 are the flexure legs combined (either the same or different ones) to compliant mechanism concepts. The number of translational and rotational DoFs are here defined as; $i\boldsymbol{T}$ and $j\boldsymbol{R}$ for the end-effector mobility $\mathcal{F}_e$, and as $k\boldsymbol{T}$ and $l\boldsymbol{R}$ for the kinematic solutions $\mathcal{F}_i$, whereby i, j, k, l are counters.

As shown in Fig. 1 the first step of the COMAD method results in a variety of kinematic solutions for a required motion pattern, $\mathcal{F}_e$. Here the different types of legs are named as legtype-1, $\mathcal{F}_{l1}$, legtype-2, $\mathcal{F}_{l2}$, etc. up to legtype-*n*, $\mathcal{F}_{ln}$, and their topologies are succinctly described by the set of DoFs provided by the prismatic and revolute joints in the linkage, i.e. the number k_i of T DoFs and the number l_i of R DoFs in the leg, respectively. As illustrated by the two branches in Fig. 1, not only the types of legs are different but also the obtained mechanisms; a serial mechanism for the one type of leg with the same set of DoFs as the end-effector, i.e. $i = k_1$ and $j = l_1$ such that solely one leg is sufficing or parallel mechanism when full mechanism concepts are assembled by a set of legs in parallel.

As example, Fig. 2 shows two full mechanisms for a Schönflies motion, $\mathcal{F}_e = 3\boldsymbol{T}{-}1\boldsymbol{R}$, assembled using two different kinematic solutions. For illustrative purposes, these are already assembled to full rigid body mechanisms something that has not been done in step 1 of the COMAD method yet. On the left of Fig. 2 is a serial mechanism shown comprising one leg and on the right is a parallel mechanism shown with a set of two similar legs in parallel. Among many other leg types, these two kinematic solutions can be found in Table 9.1 on page 150 of [18] for a Schönfies motion and the associated geometrical conditions are there documented too. The leg in the left mechanism is described there as *3R-1P* and the two legs in the right mechanism are described there as *2R-2P*. Here they are called legtype 1, $\mathcal{F}_{l1} = 3\boldsymbol{T}{-}1\boldsymbol{R}$, and legtype 2 $\mathcal{F}_{l2} = 2\boldsymbol{T}{-}2\boldsymbol{R}$, i.e. a serial linkage with three prismatic joints (P_1, P_2, P_3) and one revolute joint $(R_1,)$ and a serial linkage with two prismatic joints (P_1, P_2) and two revolute joints (R_1, R_2). The first one is a serial kinematic solution hence only one leg is required for assembling a full mechanism, whereas the second one is a parallel kinematic solution hence multiple legs in parallel are required to connect the end effector.

Step 2: Flexure leg synthesis

In step 2 of the COMAD method, the kinematic solutions of step 1 are transformed into a compliant flexure leg by means of the FACT method [2,14,15]. This method consists of the so-called 'FACT-library of freedom and constraint-spaces' wherein 26 complementary pairs of freedom- and constraint-spaces are listed that can be used to obtain multi-DoF compliant mechanisms with parallel flexures connecting an end-effector with the desired set of DoFs. The library has six columns whereby each column contains freedom spaces with the same number of DoFs, ascending from 0 to 5 DoF (counting from left to right). Each cell (counting

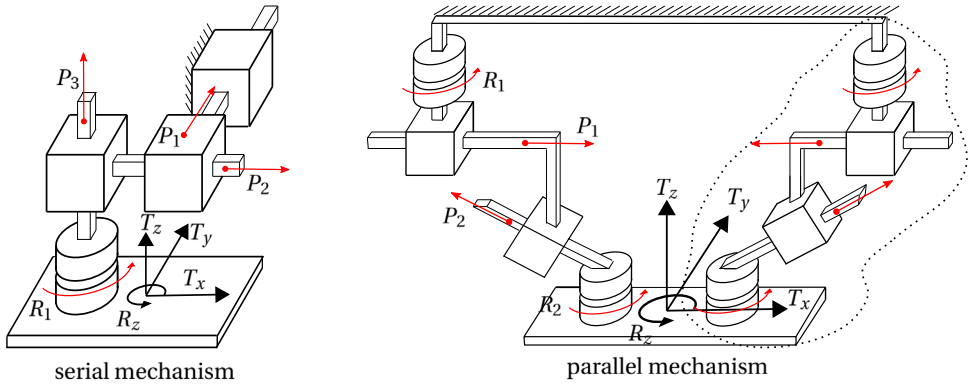

Fig. 2. Two types of kinematic solutions; both for a Schönflies motion generator. On the left, a serial mechanism which is an open mechanical linkage connecting the end-effector. On the right, a parallel mechanism which is a closed mechanical linkage with multiple legs in parallel.

bottom-up) shows a complementary pair of freedom (left side) and constraint (right side) spaces (F/C-space-pair) that is noted here as '**XDOF-y**', where **X** pertains to column number and **y** to the row. In a freedom-space are the axes of the permitted rotational DoFs given by a red line and the permitted translational directions by a black arrow (or perpendicular to a red circle). The directions in which a rigid body can/must be constrained by wire flexures are given in the constraint space by blue lines or planes.

Each kinematic solution is an open serial mechanical linkage and is transformed into a flexure leg concept by first attempting to identify a single freedom space that contains the same set of DoFs as the considered leg type. Then must be checked if all its DoFs do satisfy the geometrical conditions associated with the leg. When fulfilled, then a correct freedom space has been found and a flexure leg of a single topology can be synthesized by selecting enough non-redundant constraints from its complementary constraint space.

If no correct freedom-space has been found, then in the second attempt, first the set of DoFs of the considered leg type must be split into parts whereafter flexure leg concepts of multiple serial topologies can be obtained via the same procedure described in [20] for serial flexure systems. The leg's DoFs can be divided and paired as different subsets; i.e. a pair can have a different number N of the subsets but also the size of the subsets can be alternated (the number of DoFs per subset). Then for each pair DoFs must be identified if all its subsets do have matching freedom spaces in the FACT library. Subsequently, it must be checked if the found freedom spaces are correct by checking if all DoFs within a freedom space do satisfy the geometrical conditions but also if they are able to be satisfied among each other. The latter could result in certain orientation constraints for particular topologies. When found and fulfilled, then finally a flexure leg concept of multiple topologies in series can be synthesized by selecting enough non-redundant constraints from each of its complementary constraint spaces.

Step 3: Assembly to obtain compliant mechanism concepts

In step 3, full compliant mechanism designs are obtained by connecting the end-effector with flexure legs in parallel to the base. The assembly consists of different steps; first, the location of the base and the end-effector relative to each other must be determined. Subsequently, the number and type of flexure legs must be selected and they must be assembled correctly.

The flexure legs are designed independently hence the selection can be as desired. The number of legs can be one when selecting a flexure leg originating from the serial kinematic solution, else multiple flexure legs need to be combined in parallel, either the same legs or different ones, as illustrated in the mechanisms sketches (a) till (e) at the bottom of Fig. 1.

For the assembly, the flexure legs must be placed parallel in between the end-effector and the base. For the relative position, orientation, and order of the leg's topologies to each other, and the position and orientation of the flexure legs relative to the end-effector, anything is permitted as long as their internal DoFs satisfy the geometrical conditions related to the initial leg type. Once connected, both legs are kinematically coupled to each other. Their mobility is identical to the initial leg types, so their coupling was already taken into account.

As an example, if a flexure leg originates from the given legtype 2 in step 1 then its internal DoFs need to satisfy the same geometrical conditions as provided for the joints of legtype 2 documented on page 150 of [18]. There is stated that; all rotational axes of the legs R-DoFs must be parallel with the intended rotational axis of the end-effector and that the direction of at least one of the legs T-DoF is not perpendicular to them. As can be seen in Fig. 2, those geometrical conditions are satisfied by both legs in the right rigid body mechanism. So, for assembling two flexure legs originating from legtype 2, any position and orientation of the legs and their topologies are permitted as long as one ensures that the rotational and translational lines do satisfy the same stated conditions. Only then are their internal DoFs correctly coupled to each other resulting in a movable mechanism with the desired end-effector motion.

Finally, the shapes of the end-effector and the intermediate rigid bodies for serial topologies must be designed and fully compliant mechanism designs are obtained.

Table 1
Resulting from step 1: the 4- and 5-DoF kinematic solutions for a Schönflies motion generator $\mathcal{F}_e = 3T–1R$ [18].

4-DoF legtypes		5-DoF legtypes	
Legtype-1	$\mathcal{F}_{l1} = 3T–1R$	Legtype-4	$\mathcal{F}_{l4} = 3T–2R$
Legtype-2	$\mathcal{F}_{l2} = 2T–2R$	Legtype-5	$\mathcal{F}_{l5} = 2T–3R$
Legtype-3	$\mathcal{F}_{l3} = 1T–3R$	Legtype-6	$\mathcal{F}_{l6} = 1T–4R$
		Legtype-7	$\mathcal{F}_{l7} = 5R$

Table 2
Results of step 2, attempt one; shown per column downwards for each of the three 4-DoF legtypes of step 1 that are proceeding the synthesis process. The two bottom rows show that transforming the leg's entire set of DoFs at once in one compliant topology has not resulted in a flexure leg.

Desired end-e. set of DoFs	$\mathcal{F}_e = 3T–1R$		
	↓	↓	↓
Possible 4-DoF legtypes	Legtype-1	Legtype-2	Legtype-3
Leg's set of DoFs	$3T–1R$	$2T–2R$	$1T–3R$
F/C-space pair(s)	×	**4DOF-2**	**4DOF-(1,3)**
Geo. cond. are met	×	×	×

3. Design example: A compliant Schönflies motion generator

To illustrate the COMAD method it is applied for the synthesis of flexure legs for a Schönflies motion generator and assembling a full parallel compliant design. The end-effector of a Schönflies motion generator can translate in all three dimensions of a Cartesian coordinate system and has one rotation around an axis with a fixed direction [18], which is set in the vertical direction in this example. The intended set of end-effector DoFs can thus be defined by three translational DoFs and one rotational DoF, $\mathcal{F}_e = 3T–1R$.

Step 1: Kinematic leg solutions

The kinematic solutions for a Schönflies motion pattern can be found in table 9.1 on page 150 of [18] and are shown here in Table 1; three types of legs with 4-DoFs and four types of legs with 5-DoFs. In the continuance of this example are only the 4-DoFs legtypes included for the brevity of the design process, so legtypes 1, 2 and, 3 proceed in steps 2 and 3. The serial kinematic solution is legtype 1 (already shown in Fig. 2(a)) as it has the same set of DoFs as the end-effector.

The two geometrical conditions associated with legtype 1, 2, and 3 are listed below. Here, geometrical condition 1 (G1) imposes that all rotational axes of the R-DoFs must always be in parallel in a flexure leg during steps 1 and 2. For step 3 it determines that all rotational axes of the R-DoFs of the mechanism must be parallel with the intended rotational axis of the end-effector as for these legtypes are the R's in Table 9.1 of [18] are denoted as R̂. Geometrical condition 2 (G2) imposes that at least one of the T-DoFs of each leg is not perpendicular to the rotational axes.

(G1) The axes of all R-DoFs are always parallel
(G2) The direction of at least one T-DoF is not perpendicular to the axes of the R-DoFs.

Step 2: Flexure leg synthesis

Table 2 presents per column the results of the first attempt to identify a correct single freedom-space for each leg type. A leg has four DoFs so the **4DOF**-column of the FACT-library was used to identify a freedom-space with the same DoFs as the leg. The name(s) of F/C-space-pair(s) with equal DoFs were listed once found or marked with an '×' if not. It can be seen that for legtype 1 no equal F/C-space-pair was identified, that legtype 2 has the same DoFs as F/C-space-pair **4DOF-2**, and that legtype 3 has the same set of DoFs as both F/C-space-pair **4DOF-1** and **4DOF-3**. However, none of them is a correct freedom-space as the geometrical conditions were not met since each of the freedom spaces contained rotational axes that are not parallel. Consequently, no 4-DoF flexure leg of a single topology can be obtained for a Schönflies motion generator.

Thence, in the second attempt must be endeavored to synthesize flexure legs of multiple serial topologies for each leg. Hereby, are we first aiming for just $N = 2$ topologies. Table 3 presents the results of legtype 1, 2, and 3 in subtables (a), (b), and (c), respectively. At the top of each subtable are the four DoFs of each legtype listed and in the columns underneath are the results shown for the different distributions of them among pairs having two subsets. Two alternatives were possible for the size of these subsets; the four DoF can either be split in a pair that has two subsets with both sizes of 2-DoF or split in a pair that has a subset with a size of 3-DoF plus a subset with a size of 1-DoF. Underneath the pairs are the results shown of the sequential steps of the synthesis process.

Table 3(a) shows that the distribution of the DoFs of legtype 1 resulting in three different pairs and that finally only one of them result in a flexure leg concept. Only for pair-3 were freedom-spaces found with same DoFs as each of its subsets; F/C-space-pair **3DOF-2** and **1DOF-3**. This combination is a correct combination of F/C-space-pairs as both geometrical conditions are satisfied within and among them as long as their translational DoFs were not aligned. So, legtype 1 results in one flexure leg concept with

Table 3
Results of step 2, attempt two; aiming for flexure legs of two serial topologies for the three 4-DoF legtypes, for which the results are listed in subtable (a), (b), and (c), respectively. Presented column-wise, the resulting pairs of spliting the leg's set of DoFs into two subsets and transforming them into compliant topologies. As seen in the bottom row, we found five pairs of topologies that can be used in series as flexure leg designs: the ones resulting from pair-3 of legtype-1 and the four resulting from pair-1 of legtype-2.

	(a)			(b)				(c)		
Leg's set of DoFs	$\mathcal{T}_{l1} = 3T{-}1R$			$\mathcal{T}_{l2} = 2T{-}2R$				$\mathcal{T}_{l3} = 1T{-}3R$		
	↓ Pair-1	↓ Pair-2	↓ Pair-3	↓ Pair-1	↓ Pair-2	↓ Pair-3	↓ Pair-4	↓ Pair-1	↓ Pair-2	↓ Pair-3
Resulting subsets of DoFs	***(TT)*** ***(TR)***	***(TTT)*** ***(R)***	***(TTR)*** ***(T)***	***(TR)*** ***(TR)***	***(TT)*** ***(RR)***	***(TTR)*** ***(R)***	***(TRR)*** ***(T)***	***(TR)*** ***(RR)***	***(RRR)*** ***(T)***	***(TRR)*** ***(R)***
F/C-space pair(s)	×	×	**3DOF-2** **1DOF-3**	**2DOF-(2,8,9)**	×	**3DOF-2** **1DOF-1**	**3DOF-1** **1DOF-3**	**2DOF-(..)** **2DOF-1**	**3DOF-(3,8)** **1DOF-3**	**3DOF-(..)** **1DOF-3**
Geo. con. are met	×	×	✓	$\checkmark^{*}_{(4/6)}$	×	×	×	×	×	×

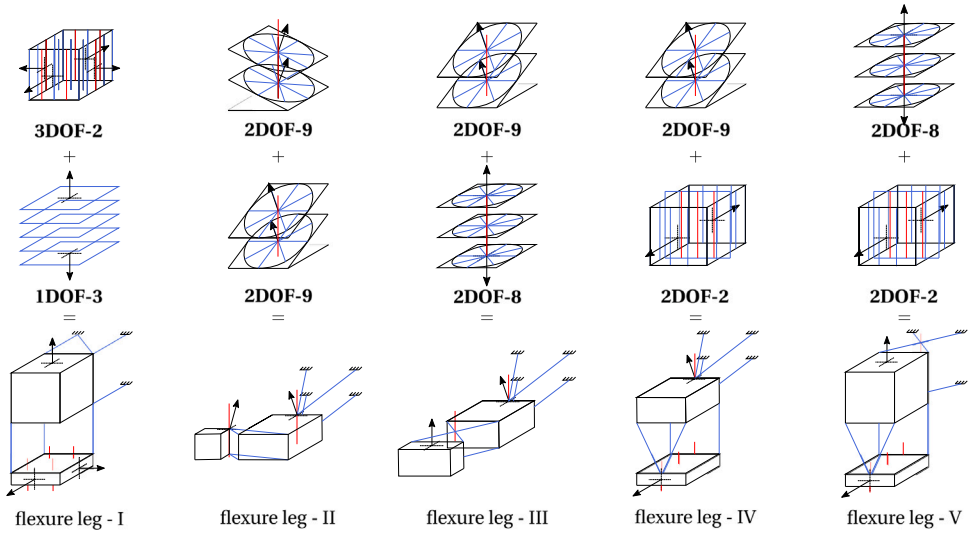

Fig. 3. Resulting flexure legs: In rows 1 and 2 are the F/C-spaces listed for each leg and row 3 presents an example of an assembly of a full flexure leg design.

those two topologies in series. This flexure leg is, called *flexure leg-I* and is visualized in the first column of Fig. 3. In the first and second rows of the figure are the two correct pairs of F/C-spaces shown (the F/C-spaces are joined within a single volume block) and in the third row, an example of the synthesized flexure leg is presented by selecting four non-redundant constraints per constraint-space.

Table 3(b) shows four pairs with different distributions of the DoFs of legtype 2 and how finally pair-1 results in four different flexure leg concepts. Pair-1 has two identical subsets each with one T- and one R-DoF. Three F/C-space-pairs contain one T-plus one R-DoF hence matching the subsets, namely **2DOF-2**, **2DOF-8**, and **2DOF-9**. Consequently, pair-1 can be assembled in six different ways by combining each F/C-space-pair with itself or with one of the other two. Four of them are correct combinations of F/C-space-pairs because they can satisfy both geometrical conditions within and among them: a combination of (**2DOF-9**)(**2DOF-9**), of (**2DOF-9**)(**2DOF-8**), of (**2DOF-9**)(**2DOF-2**), and of (**2DOF-8**)(**2DOF-2**). They are a correction combination of F/C-space-pairs as long as the rotational axes of both freedom spaces are aligned and, when relevant, the T-DoF of **2DOF-9** is not aligned with the T-DoF of the second pair. The other two combinations with **(2DOF2)(2DOF2)** and with **(2DOF8)(2DOF8)**, were rejected because both geometrical conditions cannot be satisfied simultaneously. The other pairs did not result in flexure leg concept. For pair-2 were no F/C-space-pairs were found and for pair-3 and pair-4 were F/C-space-pairs found but they were not correct because they cannot satisfy both geometrical conditions simultaneously. Altogether, legtype 2 has resulted in four different flexure leg concepts of two serial topologies which are visualized at the second till the fifth column of Fig. 3 and called *flexure leg-II* till *flexure leg-V*, respectively.

Table 3(c) shows that no flexure legs were found for legtype-3 because all of its pairs did require a freedom space with multiple R-DoFs for one of its subsets. Although multiple F/C-space-pairs did contain multiple R-DoFs, none of had them with the rotational axes in parallel and consequently all breaking with geometrical condition-1.

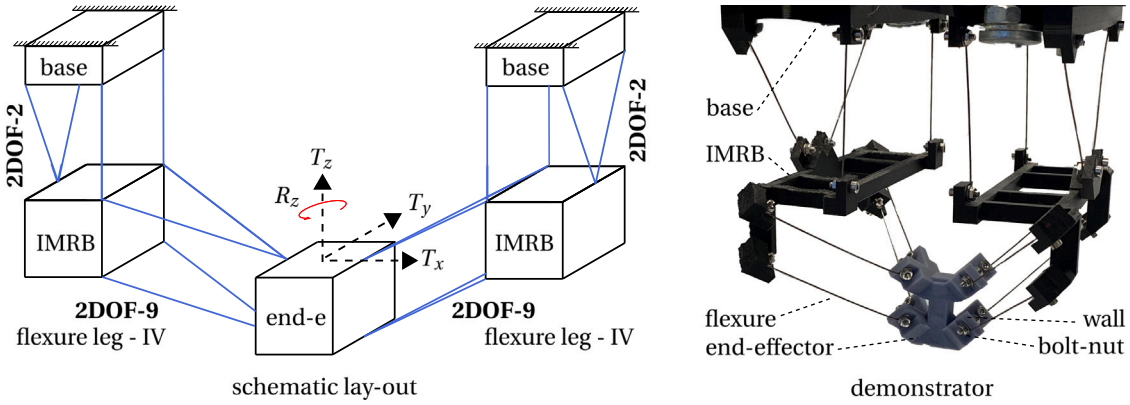

Fig. 4. A compliant Schönflies motion generator design: a 4-DoF parallel compliant mechanism assembled with two flexure legs-IV designs. On the left, the theoretical layout of the design by connecting F/C-space **2DOF-2** with the base and **2DOF-9** with the end-effector and interconnecting them with an intermediate rigid body (IMRB) in each leg. On the right, the manufactured demonstrator with 3D-printed rigid bodies connected by spring steel wire flexures.

Step 3: Assembly to obtain compliant mechanism concepts

On the left of Fig. 4 is an assembly of a full parallel compliant design with a Schönflies motion presented that has two flexure legs. For both legs was the same *Flexure legs-IV* design selected and combined in parallel at either side of the end-effector. It was determined that the base of the mechanism was located at the ceiling and the end-effector placed underneath it. In between them are the intermediate bodies (IMRB) located and are connecting both serial topologies of the legs. Towards the end-effector was topology **2DOF-9** connected at the crossing point of its wires and topology **2DOF-2** was connected with the base. Both were orientated such that all rotational axes were aligned in the vertical direction. Finally, they have positioned such that their wires were not within the same volume and a symmetrical design around the yz-plane of the end-effector was obtained. When a different design is desired; without violating the geometrical conditions, the order of topologies can be reversed, and/or they can be rotated in the xy-plane, and/or they can be moved around in space, and/or the base and intermediate bodies could be located differently relative to the end-effector. In addition, one could also use multiple or different flexure leg designs instead of the current two.

4. Demonstrator model

On the right of Fig. 4 is the manufactured demonstrator model shown of the parallel compliant mechanism that was synthesized in Section 3. The end-effector, the intermediate rigid bodies (IMRBs), and the base connections were 3D-printed of PLA material and were shaped such that the wires could be connected. The distance between the base and the IMRBs is 100 mm in the vertical direction and the distance between the end-effector and the IMRBs is 100 mm in the horizontal and 100 mm in the vertical direction. The wires were manufactured by cutting thin rods into lengths of 104 mm for the vertical ones and in lengths of 146 mm for the diagonal ones. The rods have a diameter of 3 mm and are made of stainless spring steel 1.4310 (AISI 301).

For the assembly were 2 mm deep holes drilled into the rigid body parts such that the wires can partly be inserted. Next to this connection point was a rigid wall printed along with the rigid body in the longitudinal direction of the wire. The wires and rigid parts were fixed using an M3 bolt-nut connection that clamps the side of each wire against the side of the wall.

5. Experimental set-up

The DoFs of the demonstrator will be evaluated using its eigenmodes through experiments. For this, the experimental set-up presented in Fig. 5 has been built. The base of the demonstrator was suspended by 4 wires to float freely and was excited by an electrodynamic shaker with a frequency sweep from 2 to 50 Hz which was generated by a "Brüel & Kjear Vibration exciter type 4809". The input function was a sinusoidal function with an amplitude of 1.5 V whereby the frequency was manually increased with step sizes of 0.1 Hz and was generated by a "Keysight 33220A function generator".

The entire experiment was recorded, and the resulting vibrations are the eigenmodes of the demonstrator. Those that appear at relatively low frequency are the DoFs of the demonstrator because the stiffness in these directions, K_D, is relatively low compared to the other constraint directions, K_c. An approximation of the stiffness ratio between the constraint and DoF direction $K_{c/D}$ can be calculated using Eq. (1). Here, ω_D^2 is the eigenfrequency of a potential DoF and ω_c^2 the eigenfrequency of an higher eigenmode or the maximum frequency value of the sweep when comparing it with the stiffness in a direction where no eigenmode has been observed. This equation was derived from the formula for the natural eigenfrequency of a mass–spring system where it was assumed that the mass or inertia term of the end-effector is equal in the DoF and constraint direction.

Two straight bars were attached to either side of the end-effector for better visualization of the motions. The bars are hollow, weigh 26 g, and have a length of 75 mm. Two different experiments have been done, as shown in Fig. 5, to approximately equalize

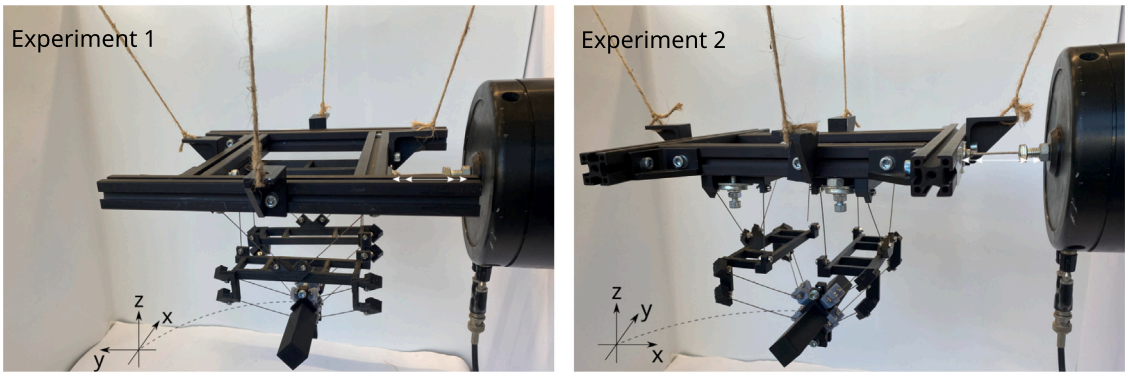

Fig. 5. The experimental setup: to evaluate the DoFs of the demonstrator using its eigenmodes. For this, its base was suspended by 4 wires to float freely and excited by an electrodynamic shaker from 2 to 50 Hz, represented here by the white two-headed arrow. The eigenmodes of the manipulator become visible and were recorded. They represent the distinctive DoFs of the compliant manipulator for which the stiffness of the design is relatively low. For better visualization of the motions were two hollow bars attached at either side of the end-effector. To equalize the added inertia, the experiment was performed twice with the difference that the demonstrator has been rotated 90° in the suspension and the bars were mounted on the other facets.

Table 4
The results of experiment 1 and 2: three translational motion and one rotation in the horizontal plane became visible during the first four eigenmodes and they are the DoFs of the demonstrator. The first eigenmode beyond them was observed at 44 Hz as a rotation around the x-axis.

Motion of the eigenmodes	Eigen frequencies in experiment 1 [Hz]	Eigen frequencies in experiment 2 [Hz]
T_x	10.8	10.8
T_y	14.5	14.3
T_z	16.7	16.7
R_z	18.5	17.9
R_x	N/A	44.0

the added inertia about the x, y, z-axes. In both experiments, the bars are pointing perpendicular to the excitation directions of the shaker, however, the demonstrator has been rotated 90° in the suspension comparing experiment 1 with 2.

$$K_{c/D} = \frac{K_c}{K_D} = \frac{\omega_c^2}{\omega_D^2} \tag{1}$$

6. Results

The entire recording of experiment 1 can be seen in the video provided in the supplementary files of this article, called "COMADmovie.mp4". Here, the eigenmodes of the demonstrator become visible. Table 4 presents the displacement of the motions and the eigenfrequency values of both experiments 1 and 2. Each of the motions did appear separately and were starting and damping out a few tenths of Hz before/after the listed frequency values.

The first 4 eigenmodes were in a frequency range from 10.8 to 17.9 Hz in experiment 1 and from 10.8 to 18.5 Hz in experiment 2, and visualized in Fig. 6. They had the same motion, 3 translations along the x,y,z-axis, and 1 rotation in the horizontal plane. Each of the motions did emerge around approximately the same frequency value in both experiments.

The first 4 eigenmodes represent the distinctive DoFs of the compliant manipulator because the stiffness of the design is relatively low compared to other directions. The linear stiffnesses of the translational DoFs are of comparable size and at least 9 times smaller than in any other direction as no other translating eigenmodes were observed. The rotational DoF around the z-axis has a rotational stiffness that is at least 7.5 times smaller than around any other axis, with the exception of the x-axis. Here, the first eigenmode beyond the 4-DoFs was observed in experiment 1 at a significantly higher frequency of 44 Hz. This eigenmode was a rotational motion around the x-axis, with a rotational stiffness of approximately 6 times higher than rotational DoF around the z-axis.

7. Discussion

Experimental results

The mobility of the demonstrator has successfully evaluated during the experiment for two reasons. At first, the first four eigenmodes of the demonstrator are the four intended motions of the Schönflies motion pattern and were observed in both experiments. Secondly, they are the DoFs of the compliant mechanism as their stiffness is significantly lower than in other directions.

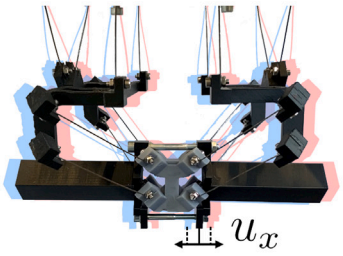

(a) Displacement u_x in direction of T_x DoF

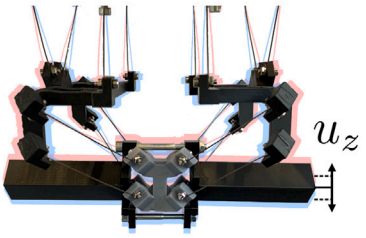

(b) Displacement u_z in direction of T_z DoF

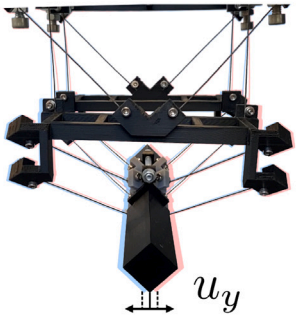

(c) Displacement u_y in direction of T_y DoF

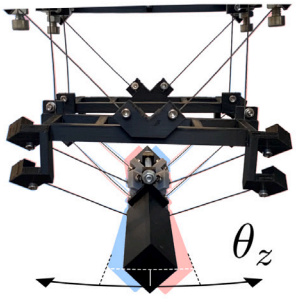

(d) Rotational displacement θ_z in direction of R_z DoF

Fig. 6. Experimental results: the three translational displacements and the rotational displacement during the first four eigenmodes.

Although the rotational stiffness around the x-axis was already 6 times larger than that around the z-axis, it could be increased in the future by rearranging the flexures of topology **2DOF-9**. The current choice to connect them nearby the x-axis of the end-effector is far from optimal to prevent a rotation around the x-axis. The resulting moment to counteract this rotation is relatively small and could be increased by, for instance, arranging the flexures in an X-shape instead of the current V-shape orientation.

The few tenths of a Hz difference in the eigenfrequency values of u_y and θ_z between experiments 1 and 2 can be caused by a difference in the moment of rotational inertia. The end-effector is wider in the x-than in the y-direction and thus are the bars differently located regarding the center-line of the end-effector. The u_y and θ_z motion involve rotating movements of the mechanism's rigid bodies hence their eigenfrequency values change by this difference while the eigenfrequency values of the u_x and u_z motion remain unchanged.

Mechanism design results

In principle, it is possible to synthesize all types of serial and parallel multi-DoF compliant mechanisms using the COMAD method. The COMAD method is established upon two classical methods i.e. 'the type synthesis of legs'-method and the FACT method. With the former, all types of legs can be found for a particular motion pattern such that in principle all rigid body mechanisms, either serial or parallel, can be constructed by combining multiple legs in parallel. Till now, it was not possible to use the FACT method to transform those closed loop rigid body mechanisms into compliant flexure mechanisms as it is directly applied to the desired end effector motion. In the COMAD method, we apply the FACT method to the individual leg types that were obtained as intermediate results by first using the legtype synthesis process for the required motion pattern. That is possible because they are open serial kinematic chains with a set of DoFs. For each of them, all flexure mechanisms that exist can be found using the FACT method since they documented all single flexure topologies that could be achieved for 26 different sets of DoFs and they had mathematically proven that they found them all. If excluded from those 26 DoFs, then a flexure solution was constructed by stacking multiple of those 26 topologies in series. Consequently, all types of serial and parallel multi-DoF compliant mechanisms can be synthesized for a required motion pattern using the COMAD method because all kinematic solutions and all possible flexure legs are included and finally the results can be assembled together into full compliant designs.

It has been shown in Section 3 of this article that with the COMAD method indeed a variety of multi-DoF compliant mechanism designs were found. The obtained solutions included the design that would have been got with the FACT method, namely flexure leg-I, i.e. the serial kinematic solution. Additionally, another four 4-DoF flexure legs-II, -III, -IV, -V were found, and combining them result in different parallel compliant mechanism designs that would have remained unnoticed till now. Furthermore, significantly more flexure legs were obtained in the presented design case if also the 5-DoF leg types were included. In general, those 5-DoF leg

types contain more R-DoFs than 4-DoF legtypes but that does not immediately request flexure legs with more than 2 topologies. Unlike the R-DoFs of the 4-DoF legtypes in Section 3, some of the 5-DoF legtypes do not request that all the axes of its R-DoFs must be in parallel but only a subset of them. For example, legtype-6 $\mathcal{F}_{l6} = \boldsymbol{1T\text{–}4R}$ is noted in [18] as a combination of 1-P with 2-$\tilde{\acute{R}}$ and 2-$\acute{R}$, e.g. P$\tilde{\text{R}}\acute{\text{R}}\acute{\text{R}}\tilde{\text{R}}$, what means that only those R-DoFs with the same superscript need to have parallel rotational axes. As a result, legtype-6 can be combined into a flexure leg of two topologies by grouping together the non-parallel R-DoFs in an F/C-space.

COMAD method steps

One additional action needs to be added to step 3 of the COMAD method to get exact constrained compliant mechanism designs, namely; the number of constraints acting in the entire mechanism needs to be recalculated. Now, exact constraint flexure legs are obtained in step 2 but by assembling them in parallel the resulting design will be over-constrained. The 4-DoF demonstrator, for instance, has three rigid bodies so 18 initials DoFs and sixteen wires hence sixteen constraints resulting that the system being over-constrained by two. By recalculating the constraints active on each rigid body of the mechanism, two arbitrary wires connected to the end-effector must be removed to achieve an exact-constrained design.

Further research

It is interesting for future research to compare the mechanical behavior of multi-DoF parallel compliant mechanisms with that of multi-DoF serial compliant mechanisms. Generally, both have multiple serially stacked topologies but there is a difference in how they deform during motion which in all likelihood results in different mechanical behavior. For a serial mechanism always one topology deforms while the other topology remains undeformed because each end-effector DoF is caused by the deformation of the same internal DoF. On the other hand, certain DoFs of parallel compliant mechanisms are related to multiple, often different, DoFs within the mechanism resulting in deformations of multiple of its serial flexure topologies. As an example, this can be observed for the demonstrator's DoFs u_y, u_z, and θ_z as they were accompanied by a simultaneous deflection of both serial topologies in a leg.

The difference in deformation of serial and parallel mechanisms is probably resulting in different mechanical behavior. Consider, for instance, the added deflection of two serially stacked topologies and the internal reaction forces which arise between the legs of a parallel mechanism something that does not occur, or differently, in serial mechanisms. This probably affects the parasitic end-effector motions or their range of motion for example. Therefore, for further research, it is interesting to investigate the mechanical behaviors of multi-DoF serial and parallel compliant mechanisms and make a quantitative comparison.

Another interesting further research line is regarding the actuation of the obtained compliant mechanisms as they are non-driven compliant structures. On themselves, they can provide the required mobility and constraints between two links or between the ground and a platform and thus be used as a passive joint or as a support structure in an already driven machine. However, for a variety of applications, like manipulators, it is of significant importance to provide end-effector motion by driving the structure itself. Therefore, we provided a cable-driven example in Fig. 7 to drive the synthesized 4-DoF Schönflies generator using 8 cables and 6 actuators. Each IMRB has a translational DoF along the x-axis and a rotational DoF around the z-axis. It is driven toward those directions by pulling at the connecting cables resulting in 4 DoF end-effector motion. Actuators a, b, c, and d, drive cables 1, 2, 3, and 4, and via a differential mechanism drive actuators e, and f, both cables 5 and 6, and cables 7 and 8. Translating the end-effector in respectively the downward or upwards direction is done by driving actuators a, b, c, and d, or actuators e and f. Translating toward the left or right direction is done by driving actuator e or actuator f. Translating in the backward or forward direction is done by driving actuators a, e, c, and f, or actuators b, e, d, and f. Rotating in a clockwise or counterclockwise direction is done by driving actuators b, e, c, and f, or actuators a, e, d, and f.

8. Conclusions

This article presented the COMAD method, a systematic design method for the type synthesis of all serial and parallel multi-DoF compliant mechanisms. With this method, mechanisms can be synthesized in three steps: (1) obtaining the serial and parallel rigid body kinematic solutions for an intended set of end-effector DoFs with the *type synthesis of legs*-method; (2) transforming each legtype into a multi-DoF flexure leg by using the FACT method; and (3) combining the legs to obtain the complete compliant mechanism designs.

It was shown how with the COMAD method a variety of mechanism designs could be found that were remained undiscovered with the current design methods. We achieved this by first establishing the parallel leg solutions for a required motion pattern and then – before they would become assembled to a closed kinematic chain – applying the FACT method at this stage to them. As an example, it was applied for a parallel compliant Schönflies motion generator and resulted in five 4-DoF flexure leg concepts. Particularly four of them were unique because they have different flexure topologies than the already known mechanism that could have been obtained with the FACT method. Moreover, also that design was obtained as the remaining fifth flexure leg was identical. Additionally, a larger variety of mechanism designs could be found in the future by the incorporation of 5-DoF leg types in the design process too. Lastly, the COMAD method could be applied to other multi-DoF motion patterns in a similar manner as in the example presented in this article.

The 4 DoFs of one of the obtained compliant Schönflies manipulator designs were evaluated by experiments. For this, a physical demonstrator prototype was manufactured and an experimental set-up has been built. The first four eigenmodes of the demonstrator became visible in a frequency range from 10.8 to 18.5 Hz. Their motion was in correspondence with the intended Schönflies motion; three separate translational motions in the x-, the y-, and the z-direction and one rotational motion in the horizontal plane. They represent the 4 DoFs of the compliant manipulator, as the stiffness of the design is significantly lower, thus the demonstrator's mobility was successfully evaluated.

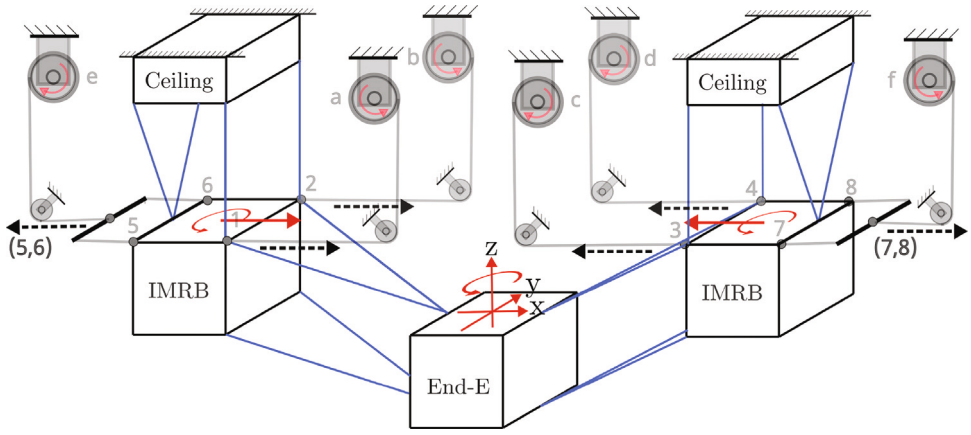

Fig. 7. Example of a cable driven compliant Schönflies motion generator to provide 3 translational and 1 rotational end-effector motion using 6 actuators, 2 differential mechanisms, and 8 cables to drive the IMRBs.

Data availability

No data was used for the research described in the article

Appendix A. Supplementary data

Supplementary material related to this article can be found online at https://doi.org/10.1016/j.mechmachtheory.2023.105342.

References

[1] L.L. Howell, Compliant Mechanisms, John Wiley & Sons, 2001.
[2] L.L. Howell, S.P. Magleby, B.M. Olsen, J. Wiley, Handbook of Compliant Mechanisms, Wiley Online Library, 2013.
[3] S. Henein, P. Spanoudakis, S. Droz, L.I. Myklebust, E. Onillon, Flexure pivot for aerospace mechanisms, in: 10th European Space Mechanisms and Tribology Symposium, San Sebastian, Spain, 2003, pp. 285–288.
[4] S.T. Smith, Flexures: Elements of Elastic Mechanisms, Crc Press, 2014.
[5] L.L. Howell, Compliant mechanisms, in: J.M. McCarthy (Ed.), 21st Century Kinematics, Springer London, London, 2013, pp. 189–216.
[6] D. Wiersma, S. Boer, R.G. Aarts, D.M. Brouwer, Design and performance optimization of large stroke spatial flexures, J. Comput. Nonlinear Dyn. 9 (1) (2014) 011016.
[7] S. Awtar, A.H. Slocum, Constraint-based design of parallel kinematic XY flexure mechanisms, 2007.
[8] H.-J. Su, D.V. Dorozhkin, J.M. Vance, A screw theory approach for the conceptual design of flexible joints for compliant mechanisms, 2009.
[9] J. Yu, S. Li, H.-j. Su, M. Culpepper, Screw theory based methodology for the deterministic type synthesis of flexure mechanisms, 2011.
[10] H. Li, G. Hao, A constraint and position identification (CPI) approach for the synthesis of decoupled spatial translational compliant parallel manipulators, Mech. Mach. Theory 90 (2015) 59–83.
[11] H. Li, Y. Liu, Z. Wang, C. Leng, Z. Zhang, G. Hao, A constraint-flow based method of synthesizing XYθ compliant parallel mechanisms with decoupled motion and actuation characteristics, Mech. Mach. Theory 178 (2022) 105085.
[12] M. Naves, M. Nijenhuis, B. Seinhorst, W. Hakvoort, D.M. Brouwer, T-flex: A fully flexure-based large range of motion precision hexapod, Precis. Eng. 72 (2021) 912–928.
[13] G. Hao, H. Li, Y.-H. Chang, C.-S. Liu, Design of four-dof compliant parallel manipulators considering maximum kinematic decoupling for fast steering mirrors, in: Actuators, 10, MDPI, 2021, p. 292, no. 11.
[14] J.B. Hopkins, M.L. Culpepper, Synthesis of multi-degree of freedom, parallel flexure system concepts via freedom and constraint topology (FACT)–Part I: Principles, Precis. Eng. 34 (2) (2010) 259–270.
[15] J.B. Hopkins, M.L. Culpepper, Synthesis of multi-degree of freedom, parallel flexure system concepts via freedom and constraint topology (FACT). Part II: Practice, Precis. Eng. 34 (2) (2010) 271–278.
[16] D. Farhadi Machekposhti, N. Tolou, J. Herder, A review on compliant joints and rigid-body constant velocity universal joints toward the design of compliant homokinetic couplings, J. Mech. Des. 137 (3) (2015) 032301.
[17] K. Folkersma, S. Boer, D. Brouwer, J. Herder, H. Soemers, A 2-DOF large stroke flexure based positioning mechanism, in: ASME 2012 International Design Engineering Technical Conferences and Computers and Information in Engineering Conference, American Society of Mechanical Engineers Digital Collection, 2012, pp. 221–228.
[18] X. Kong, C.M. Gosselin, Type Synthesis of Parallel Mechanisms, Vol. 33, Springer, 2007.
[19] D.L. Blanding, Exact Constraint: Machine Design using Kinematic Principles, Amer Society of Mechanical, 1999.
[20] J.B. Hopkins, M.L. Culpepper, Synthesis of precision serial flexure systems using freedom and constraint topologies (FACT), Precis. Eng. 35 (4) (2011) 638–649.
[21] B. Siciliano, O. Khatib, Springer Handbook of Robotics, Springer, 2016.